Vietnam Journal of Science and Technology ***64***(2) (2026) 280–291
DOI: https://doi.org/10.15625/2525-2518/18289

Reinforcement of magnetite-montmorillonite on the cathodic delamination of epoxy-based organic coating

Thu Thuy Thai[1,*], Dieu Thao Nguyen[2], Thi Thao Nguyen[1], Gia Vu Pham[1], Hoan Nguyen Xuan[2], Anh Truc Trinh[1]

[1]*Institute for Materials Science, Vietnam Academy of Science and Technology, 18 Hoang Quoc Viet, Nghia Do ward, Ha Noi, Viet Nam*
[2]*Faculty of Chemistry, VNU University of Science, 19 Le Thanh Tong, Cua Nam ward, Ha Noi, Viet Nam*

[*]Email: *ttthuy@itt.vast.vn*

Received: 21 April 2023; Accepted for publication: 24 August 2023

Abstract. This study proposes a method to reinforce the cathodic delamination capacity of organic coating on carbon steel. Epoxy-based coating containing 5 wt.% magnetite-montmorillonite particles which were prepared via co-precipitation method. The crystallization of magnetite particles *in-situ* on the surface of organo-montmorillonite were confirmed by XRD diffraction and FT-IR spectra. When used as filler in epoxy resin, the magnetite-montmorillonite-based coating showed an improvement of adhesion resulting in the reinforcement of internal strength between epoxy film and the substrate. The cathodic delamination results showed that the permeation of electrolyte through the scratch was reduced and the resistance to the cathodic disbondment was also improved. The electrochemical impedance measurements confirmed the anticorrosion improvement of the coating containing magnetite-montmorillonite particles.

Keywords: corrosion, cathodic delamination, magnetite, montmorillonite, EIS.

Classification numbers: 2.5.2, 2.5.3, 2.9.4

1. INTRODUCTION

Cathodic delamination is considered an important element promoting the lifetime of an organic coating. Many studies have been reported on this phenomenon and adhesion has become a key affecting the mechanism of the cathodic disbanding process [1, 2]. It has been demonstrated that an applied cathodic potential accelerates the cathodic reactions under the coating film, resulting in the liberation of oxygen and the loss of adhesion at the interface of metallic substrate/coating [3, 4].

It has been shown that the incorporation of pigments in the film formulation could not only promote anticorrosion properties but also hinder the disbandment phenomenon [5, 6]. Nano magnetite particles have been known as corrosion inhibitor pigments for metallic substrates in various types of applications. Our previous work reported that the incorporation of nano iron oxide Fe_3O_4 and IBA (indole-3- butyric acid) modified-Fe_3O_4 improved the properties of bisphenol A -based epoxy on carbon steel [6]. In the presence of Fe_3O_4, the blisters and the

corrosion products were limited on the surface and also around the artificial scratch after 240 h of salt spray test. The dry and wet adhesion of epoxy paint were also enhanced, due to the decrease of the adherence loss (% surface areas). This improvement can be linked to the physical bonds created by the magnetite nanoparticles and the oxide layer at the coating/carbon steel interfacial.

As the other nanoparticle pigments, the dispersion of nano magnetite into the film formulation sometimes gets difficult due to its nano size and its high specific surface energy, resulting in the limit of application. To resolve this problem, a surface modification should be applied: by organic molecules [6], by modifying their crystal lattice like cobalt-ferrite [7, 8] or by using in combination with the nanoclay as fillers. In recent years, sodium montmorillonite (NaMMT) has been used as fillers in organic coating for steel, aluminum, etc. thanks to its layered structure and reasonable price [9-11]. Several reports studied the synthesis of Fe_3O_4 nanoparticles in the lamellar structure of montmorillonite. However, due to the size and the agglomeration of magnetite particles and the application of MMTFo, the percentage of nano Fe_3O_4 in nanoclays was limited. Barraque *et al.* reported the synthesis process of magnetic-montmorillonite, via a co-precipitation method, with 5 wt.% of magnetite particles by oxidizing Fe(II) in an alkaline medium to adsorb cobalt ions [12]. A similar procedure to synthesis of superparamagnetic Fe_3O_4 in bentonite, as a possible contrast agent for MRI, was also prepared by Bartonkova *et al.* [13]. A series of size-controlled Fe_3O_4 was synthetized in the layers of MMT with the percentage varied from 1 to 12 % of mass by the co-precipitation method [14]. The higher ratio of Fe_3O_4 in the composite MMT/Fe_3O_4 (with 50 wt.% of Fe_3O_4) was only prepared by mechanical mixing of the MMT and Fe_3O_4 particles in an aqueous solution [15], not by the *in-situ* synthesis process.

In this study, nano magnetite (Fo) was *in-situ* prepared on organo-surface modified montmorillonite (MMO) layer with 50 % of mass by using the co-precipitation method. The composite MMOFo was then incorporated into an epoxy formulation as filler. The aim of this study is to evaluate the reinforcement of MMOFo on the corrosion properties, focusing on the cathodic delamination of epoxy resin coated on carbon steel. The electrochemical impedance measurements are combined with applied cathodic potential accelerated test and adhesion tests.

2. MATERIALS AND METHODS

2.1. Materials

The carbon steel substrates (15 x 10 x 0.2 cm) were abraded with SiC papers from the grade of 100 to 1200, followed by washed with ethanol absolute before application. The Organo-surface modified montmorillonite (MMO) (with containing 15-35 % octadecylamine and 0.5-5 % aminopropyltriethoxysilane) from Sigma Aldrich were used as received. The magnetite (Fo) particles were synthetized via co-precipitation method by using $FeSO_4.7H_2O$ (Sigma Aldrich, 99 %), anhydrous $FeCl_3$ (Sigma Aldrich, 97 %) and NaOH (Scharlau, 97 %) without further purification.

2.2. Synthesis of magnetite-organo montmorillonite

The MMOFo particles which contain 50 wt.% Fe_3O_4 were obtained by the *in-situ* growth of magnetite in nanoclays (MMO) sheets. A suspension of nanoclays was prepared by sonicating of 7 g MMO in 200 mL of water/isopropyl alcohol mixture (5/5 ratio), followed by stirring in 20 hours. Then, under N_2 atmospheric, a mixture of iron salts Fe^{2+} (0.015 mol) and Fe^{3+} (0.03 mol) was added drop-by-drop in nanoclays suspension. After stirring in 1 hour, a 1.25 M NaOH

solution was added in order to assure that the pH reached at 13. The suspension was kept at 85 °C for 1 hour. After the reaction, the precipitated product was purified by distilled water until neutral pH, eliminated the trace of Cl^- ions by 0.1 M $AgNO_3$ solution, and then dried at 80°C for 24 hours.

2.3. Solvent-based epoxy coating preparation

Organic coating containing 5 wt.% particles (MMO, Fo, MMOFo) covered on carbon steel plates was fabricated using EPOTEC YD 011X75 (Kudo Chemical Co., Korea) epoxy with butyl acetate as solvent and Sunmide 305-70X as hardeners. The mixtures (polymer with and without particles) were applied on pre-cleaned carbon steel substrates by spin-coating equipment at the speed of 600 rpm for 20 seconds. The final film thickness after drying is about 35 µm detected by Minitest 600 Erichen meter.

2.4. Characterization methods

The crystal lattice of synthetized materials was analyzed by Bruker D8 Advance Diffractometer with CuKα radiation source (λ = 1.54060 nm) at the scan rate of 0.003°/step. The surface morphology and the distribution of nano magnetite on the surface of nanoclays layer were observed with a Hitachi S-4800 Field-Emission scanning electron microscope. The characteristic peaks related to chemical bonds of MMO and MMOFo were identified by FT-IR Nicolet IS 10 (Thermo Scientific) spectrometer.

The adhesion performance was carried out following the ASTM D3359 standard. Twelve cuts were created through the film to the steel substrate including 1 mm apart between each line with the help of an Elcometer 1542 Cross hatch adhesion tester. After removing the standard tape over the grid, the detached surface area was classified and evaluated.

The electrochemical measurements and the cathodic delamination tests of organic coating with and without fillers (Reference) on carbon steel plates were recorded by Biologic SP-300 (Biologic Science Instruments) equipment. A classical three-electrode system was chosen for measurement: a carbon steel plate with epoxy film as a working electrode, a Pt rod as a counter electrode and an Ag/AgCl/saturated KCl as a reference electrode.

The electrochemical impedance spectroscopy (EIS) was detected in frequency range from 100 kHz to 10 mHz at open circuit potential (OCP) with an amplitude of 30 mV, 8 points per decade. The electrolyte solution was 0.5 M NaCl. The fitted results were obtained with the help of ZSimWin 3.5 software.

The cathodic delamination was characterized on the sample with a scratch of 2 cm created mechanically at the surface. The electrolyte was 0.1 M Na_2SO_4 solution which not strongly accelerated the corrosion process. A cycle of cathodic delamination test was fixed at -1.2 V (vs Ag/AgCl/saturated KCl reference electrode) in 60 minutes, and then followed by 1 hour at the OCP. This cycle was repeated 5 times. After the test, the samples were carefully cleaned and then observed with the help of a digital microscope VH-Z100 (Keyence).

3. RESULTS AND DISCUSSION

3.1. Characteristics of magnetite/organo-montmorillonite

Figure 1 shows the XRD patterns of the synthetized MMOFo particles. The characteristic diffraction peaks of magnetite can be found at: 29.7°; 35.0°, 42.5°, 56.2°, and 61.7° of 2θ angle; which are indexed as (220), (311), (400), (511), and (440) planes of Fe_3O_4, in agreement with the standard XRD pattern (ICSD# 174321). Therefore, the peak indexed of montmorillonite at 5.1° can also be observed. Based on the Bragg equation, the interplanar spacing d of MMTFo is about 21.5 Å. Compared with the value standard d = 12.9 Å of sodium montmorillonite [16-18], it is confirmed the crystallization of magnetite on the surface layer of montmorillonite.

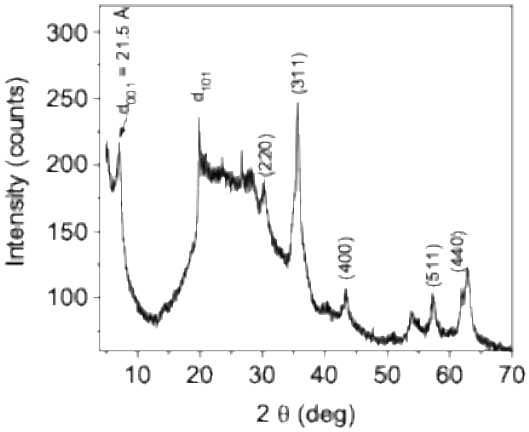

Figure 1. XRD pattern of the synthetized MMOFo.

The MMOFo surface morphology observed by FE-SEM is presented in Figure 2. The platelet structure of nanoclays can be clearly observed. On the surface of their sheets, the crystallization of magnetite can be seen visibly. The Fe_3O_4 particles seem to be spherical, their size and shape are homogenous. These images revealed the formation of Fe_3O_4 in the interlamellar and at the external surface of nanoclays sheets.

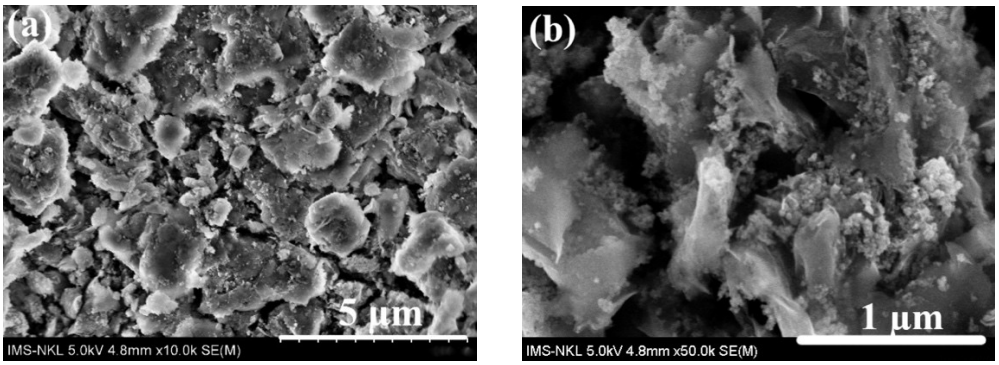

Figure 2. FE-SEM images of MMOFo.

Figure 3 reported FT-IR spectra of MMO and synthetized MMOFo particles. All characteristic peaks corresponded with chemical bonds were reported in Table 1. In FT-IR spectra of organo-clay MMO and MMOFo, the bands at 3619 – 3635 cm^{-1} are attributed to the OH^- groups

coordinated with the octahedral cations while the bands at 3443 cm^{-1} and 1635 cm^{-1} related to sketching and bending vibration mode of OH-bonds of adsorbed water. The bands around 2851-2924 cm^{-1} can be attributed to the sketching of C-H from the organic molecules modified on the surface of pristine MMO. The peaks characterized to the Fe-O bonds were well-known at 583 cm^{-1} [19]. Comparing the FT-IR spectra of MMOFo, the band around 466 cm^{-1} to 625 cm^{-1} can be attributed to the Fe-O stretching vibration but also can be due to the overlapping of Si-O-Si bonds, Al-O-Si or Si-O-Si in the nanoclays structure [14]. Therefore, the peak at 1039 cm^{-1} assigned to the Si-O bending vibration, peaks at 917 and 836 cm^{-1} related to the AlAlOH and AlMgOH sketching vibration in the interlayer sheets [20]. The results revealed that Fe_3O_4 was successfully synthetized in the structure of clay particles by creating van der Waals bonding between oxygen groups of MMO with Fe ions. There is no chemical interaction between the silicate layer and Fe_3O_4 particles.

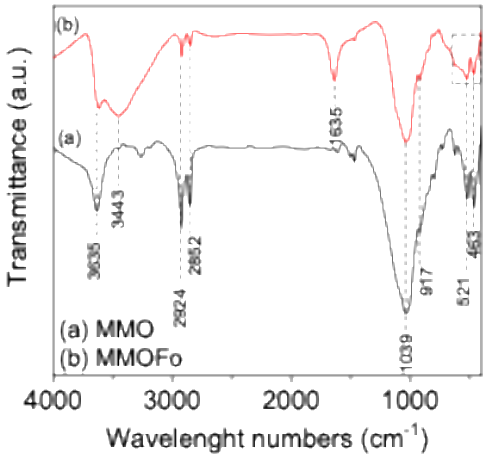

Figure 3. FT-IR spectra of (a) MMO, (b) MMOFo.

Table 1. Characteristic peak and corresponding chemical bonds of reported FT-IR spectra.

Wavelength numbers (cm^{-1})		Chemical bond
MMO	MMOFo	
3635	3619	OH- coordinated with the octahedral cations
3443	3443	OH_{ads}
2924	2921	C-H bending
2852	2851	C-H bending
	1635	$O\text{-}H_{ads}$
1039	1038	Si-O sketching
917	917	AlAlOH bending
521	522	Al-O-Si
463	463	Si-O-Si

3.2. Effects of MMOFo on the cathodic delamination of organic coating

Figure 4 represents the surface appearance of carbon steel coated epoxy layer after the adhesion examination followed by the ASTM D3359 standard. The classification of the adhesion test result is reported in Table 2. As can be observed, after the adhesion test, the removed surface

area from the substrate of the reference sample is above 28 %, Figure 4(a). Nevertheless, in the case of coating containing MMO (Figure 4(b)) and MMOFo (Figure 4(c)), the delaminated surface is less than 5 % tested surface area. This can be related to the organoclay-based pigment in the coating which contained octadecylamine and aminopropyl triethoxysilane as organic-modified surface elements. This organic content can reinforce the internal force of the coating due to the good compatibility between the pigment and the epoxy primer, so reinforcing the adhesion strength between the protective layer and the carbon steel plate.

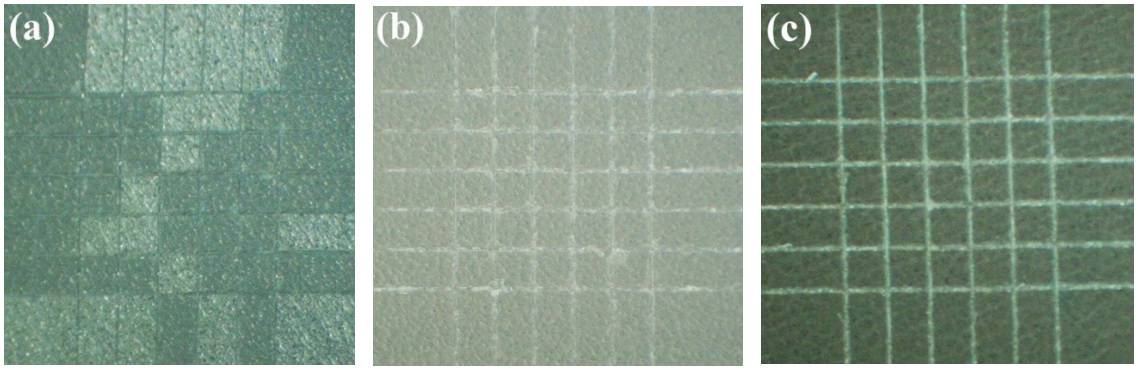

Figure 4. Adhesion performance of experimental samples followed by ASTM D3359 standard: (a) reference, (b) epoxy layer containing MMO particles, (c) epoxy layer containing MMOFo particles.

Table 2: Classification of adhesion test result based on ASTM D3359 standard.

Sample	Surface area removed (%)	Classification
Reference	~ 28 %	2B
EP-MMO	< 5 %	4B
EP-MMOFO	< 5 %	4B

The surface appearance and the disbanded epoxy layer around the scratch after cathodic delamination are shown in Figures 5-7, respectively. As can be seen, for the reference sample (Figure 5), the electrolyte solution is permeated through the scratch and visibly defined by the dashed line in Figure 5(a). As a result of the loss of adhesion, an enforced cathodic current can create a delaminated area on the epoxy surface. In this case, the unpigmented organic coating was peeled off from the carbon steel substrate, followed by the widening of the cut which was measured around 170-180 µm, Figure 5(b). The rust is also clearly observed in the cut (Figure 5(c)) that is related to the corrosion products of iron. The roughness of the surface can be observed in Figure 5(d) that is related to the removal of the epoxy layer. When added organoclay particles, MMO, into the coating formulation (Figure 6), the permeation of the electrolyte solution is reduced, which can be approved by the difficulty when detecting the permeable area (the dashed line noted in Figure 6(b)). This phenomenon is related to the exfoliating of MMO particles into the coating, which increases the diffusion path of water and aggressive elements, so retards the loss of coating properties [11, 18, 21]. In addition, the organic molecules on the MMO particles also help to improve the compatibility between clay particles and epoxy networks as a consequence of internal strength reinforcement. Moreover, the width of the artificial scratch was similar when compared to the reference sample, which was detected at around 170 µm. The rust visibly appears at the surface, Figures 6(a, c, d). This can be explained by the non-inhibitive effect of clay compound which can only increase the barrier property of the coating [18].

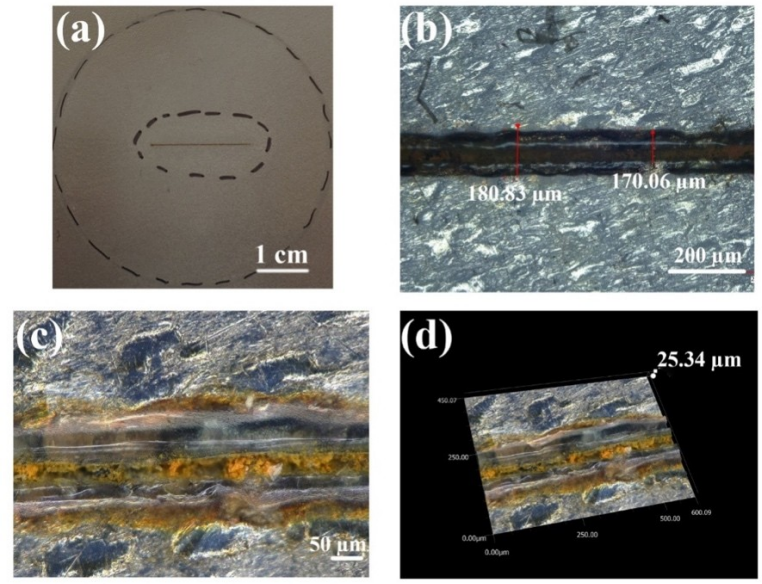

Figure 5. Surface apperance of scratched sample (carbon steel covered an epoxy layer) after cathodic delamination test.

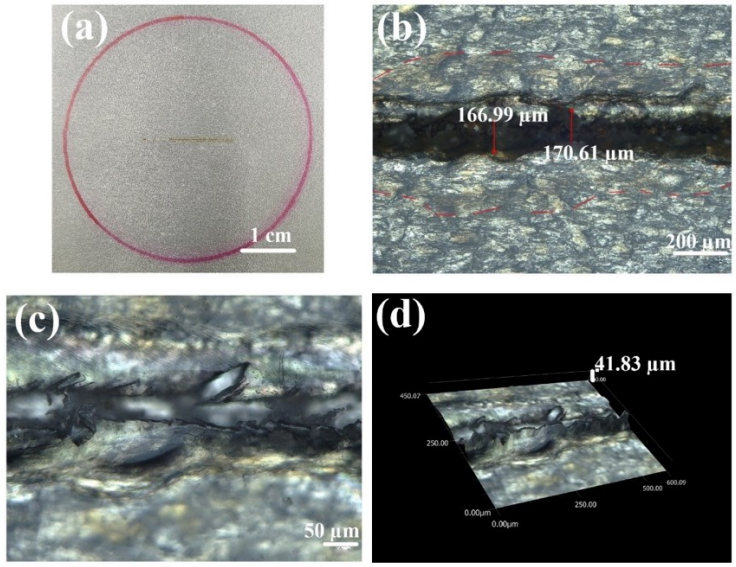

Figure 6. Surface apperance of scratched sample (carbon steel covered an epoxy layer containing MMO) after cathodic delamination test.

Figure 7 presents the surface appearance (a) and the enlarged observation of the scratch (b-d) after imposing a cathodic delamination on a MMOFo- pigmented epoxy coating. As can be observed, the delaminated surface area is significantly reduced with a fine line of scratch and no corrosion product is clearly examined, Figure 7(a). The width of the cut detected in Figure 7(b) is in the range from 60 to 80 µm which is considerably smaller than the other two. The corrosion products also appear in the scratch which is related to the film degradation in the cathodic

delamination condition. Besides that, the epoxy layer peeled off from the metallic substrate is less than the reference and the coating containing MMO. The roughness when the epoxy layer delaminated from the substrate is around 13.11 µm (Figure 7(d)), compared to the value obtained in the case of reference sample (25.34 µm) and the coating containing MMO (41.83 µm). As can be approved in many works, the cathodic polarization generated OH^- ions under the coating, leads to a local increase in pH at the delaminated area and loss of adhesion [22, 23]. Adding a filler that is able to capture OH^- ions considered as a method to prevent this phenomenon. In this work, magnetite particles play this role due to their capacity to create hydrogen bonds with OH^- ions. These generated ions can also be consumed by nano-clays particles. The more OH^- ions are consumed, the less the migration of water. In this case, this protection can be explained by the synergy effect of nanoclay that can reduce the permeation of water through the cut but also the inhibitive effect and availability of creating hydrogen bond of magnetite compound in MMOFo particles. The presence of doped particles in the coating formulation helps reduce the adhesion loss between the film and the substrate, resulting in less damage in the default.

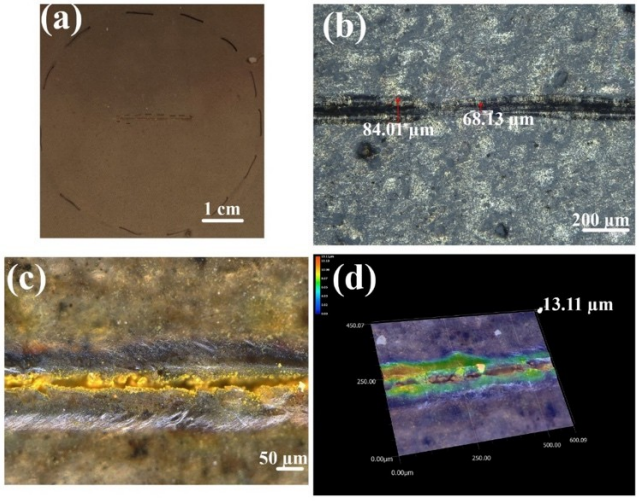

Figure 7. Surface apperance of scratched sample (carbon steel covered an epoxy layer containing MMOFo) after cathodic delamination test: (a) general view, (b-c) scratch observation in 2D mode, (d) scratch observation in 3D mode.

3.3. Reinforcement of MMOFo on the electrochemical behavior in NaCl solution

Figure 8 represents the electrochemical measurements of the carbon steel plate covered epoxy layer containing 5 wt.% doped particles (Fo, MMO, MMOFo) during immersion time in 0.5 M NaCl solution. As can be seen, at the initial immersion time, the coating containing magnetite particles presented a high modulus value in the Bode plot accompanied by a high phase angle, Figure 8(a), related to a good barrier property. Moreover, after 24 h, the modulus parameter at low frequency decreased 10 times and continuously reduced after 1 week of immersion. The second time constant clearly appeared after 1 week related to a permeation at interphase coating/ metallic substrate. When continuing the immersion, water and corrosive elements incessantly accumulated but the value of the second time constant kept stable at the end of the measurement. In parallel, the modulus values at low frequency also did not change after 7 days till 56 days of the experiment. This phenomenon is attributed to the barrier properties of the coating containing Fo that maintains the film resistance and retarded the corrosion. This trend of electrochemical

response is similar to the presence of MMO particles, Figures 8(b, b'). The modulus value at low frequency was also decreases from 10^9 to 10^7 Ω.cm^2 after 1 week of immersion with a second time constant visibly observed. Until the end of the measurement, the modulus value was slowly reduced. The incorporation of Fo and MMO particles in the formulation reinforced the barrier properties of coating at the initial immersion time and kept stably these properties for long immersion time in NaCl solution.

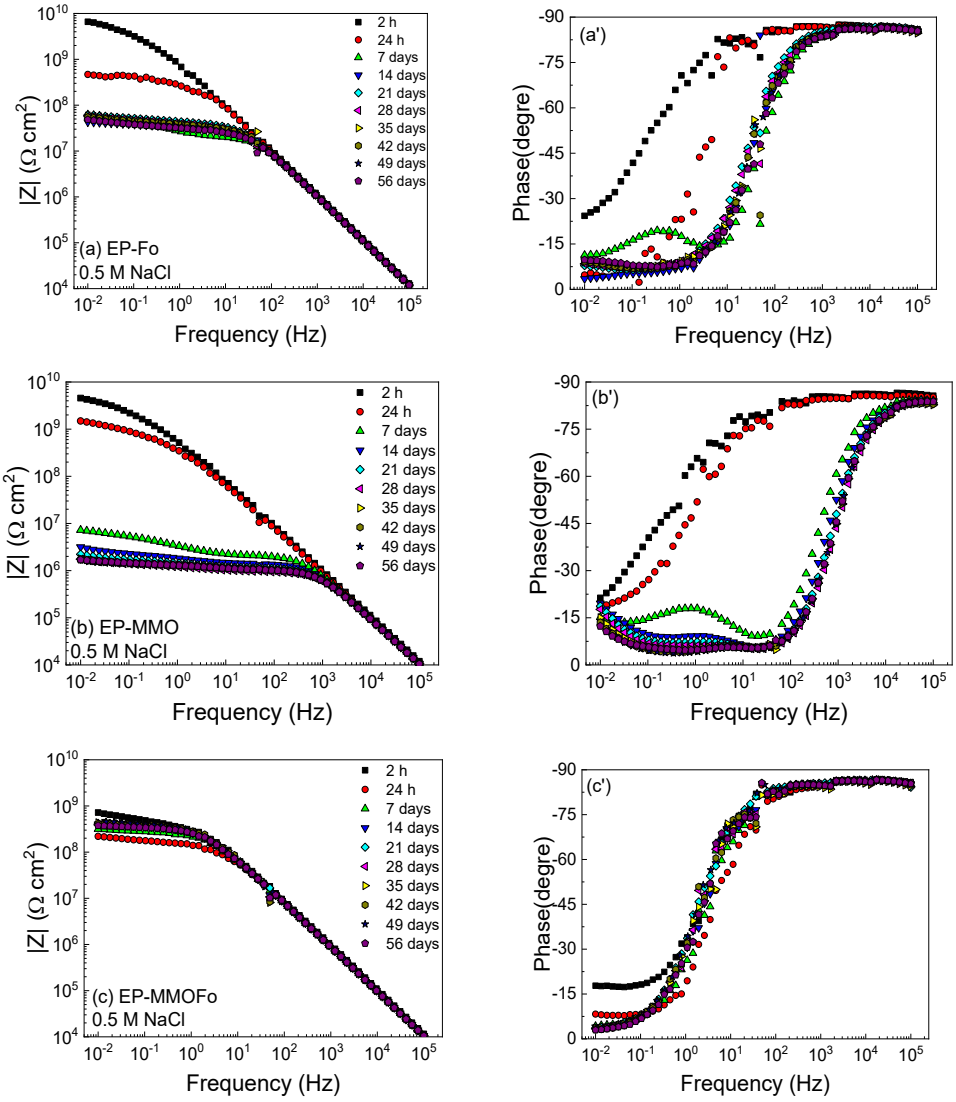

Figure 8. Bode diagrams of epoxy-based organic coating covered on carbon steel substrate during immerison time containing: (a+a') Fo, (b+b') MMO, (c+c') MMOFo.

This phenomenon is visibly improved when added magnetite- nanoclay MMOFo in the coating composition, Figures 8(c, c'). Although the modulus value at low frequency is lower than the other ones at the beginning of the measurement, this parameter is significantly unchanged during immersion time. The phase angle plot is shown one time constant at high frequency meaning a good barrier property of coating. The second time constant started appearing but is

difficult to clearly detect. In order to deepen understanding the electrochemical behavior of all experimental systems, Figure 9 presents an equivalent electrical circuit (EEC) used for modeling the obtained EIS data. R.E. and W.E. in this circuit are symbols for reference and working electrodes, respectively, while Rs is defined as the solution resistor for the case of coated metals immersed in the NaCl solution [24]; R_{coat} corresponds to the film resistor which is connected in parallel with Q_{coat} as a non-ideal capacitor of the film. R_{coat} linked in series with R_{dl} and Q_{dl}, which correspond to the double layer resistor and the non-ideal double layer capacitor. Based on this EEC, the R_{coat} and R_{dl} of each time measurement can be calculated and presented in Figures 9(b, c), respectively.

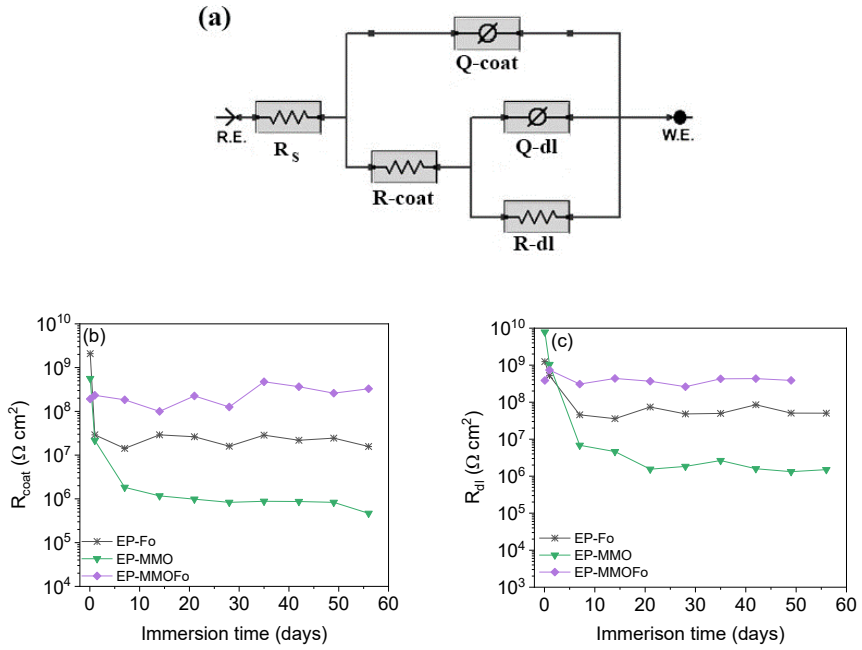

Figure 9. (a) Equivalent electrical circuit (EEC), (b) evolution of fitted R_{coat}, and (c) fitted R_{dl} following immersion time.

As can be seen, after 2 hours of immersion, the painted system containing magnetite particles (EP-Fo) and MMO particles (EP-MMO) present a high coating resistance and also a high double layer capacitance that are related to an effective barrier property, Figures 9(b, c). After 7 days of immersion, these two parameters strongly dropped about 10 to 100 times and then kept constant till the end of the measurement. On the other hand, the MMOFo-based coating hadn't showed a high coating resistance at the beginning of measurement but this factor had not changed during the long immersion time, so at the end of the measurement, this system presented an important coating resistance/double layer capacitance resistance compared to the other. These evolutions approved the effect of doped MMOFo in the epoxy coating. Although their electrochemical parameters were not too high at the initial time of test, but the coating properties remained stable during the long immersion time.

4. CONCLUSIONS

This work studied the effect of magnetite-doped organo-montmorillonite (MMOFo) on the cathodic delamination and electrochemical performance of epoxy coating covered on carbon steel. The MMOFo particles were in-situ synthetized by co-precipitation method and added in coating formulation with 5 wt.%. Compared with the reference (epoxy without pigments) and MMO-based epoxy coating, the epoxy coating containing MMOFo shows less damage in cathodic delamination which results in a reinforcement of adhesion between the epoxy primer layer and the metallic substrate. This evidence relates to the effect of organo-montmorillonite which can improve the barrier properties of the organic coating as well as the inhibitive effect of magnetite particles when doped into the epoxy layer. The electrochemical measurements also approve the improvement of MMOFo when immersed epoxy layer in NaCl solution for long immersion time. The coating resistance and the double layer resistance keep mostly constant from the beginning till the end of the measurement in which important value compared to the other experimental coating systems.

Acknowledgements. This study was supported by the Vietnam Academy of Science and Technology under grant number TĐVLTT.04/21-23.

CRediT authorship contribution statement. Thu Thuy Thai: Methodology, Investigation, Writing – original draft. Dieu Thao Nguyen: Methodology, Investigation. Thi Thao Nguyen: Methodology, Investigation. Gia Vu Pham: Investigation, Validation. Hoan Nguyen Xuan, Anh Truc Trinh: Conceptualization, Writing – review & editing.

Declaration of competing interest. The authors declare that they have no known competing financial interests or personal relationships that could have appeared to influence the work reported in this paper.

REFERENCES

1. Harun M. K., Marsh J., Lyon S. B. - The effect of surface modification on the cathodic disbondment rate of epoxy and alkyd coatings. Prog. Org. Coat., **54** (2005) 317-321. https://doi.org/10.1016/j.porgcoat.2005.07.007.
2. Deflorian F., Rossi S. - The role of ions diffusion in the cathodic delamination rate of polyester coated phosphatized steel. J. Adhes. Sci. Technol., **17**(2) (2003) 291-306. https://doi.org/10.1163/156856103762302050.
3. Balaji R., Gadhave K., Shreepathi S., Akilan V., Mallik B. P. - Investigating the role of key ingredients on cathodic delamination resistance of high-build pigmented epoxy coatings. J. Coat. Technol. Res., **10**(1) (2013) 87-95. https://doi.org/10.1007/s11998-012-9460-4.
4. Ghanbari A., Attar M. M. - The effect of zirconium-based surface treatment on the cathodic disbonding resistance of epoxy coated mild steel. Appl. Surf. Sci., **316** (2014) 429-434. https://doi.org/10.1016/j.apsusc.2014.07.178.
5. Yin Y., Zhao H., Prabhakar M., Rohwerder M. - Organic composite coatings containing mesoporous silica particles: Degradation of the SiO_2 leading to self-healing of the delaminated interface. Corros. Sci., **200** (2022) 110252. https://doi.org/10.1016/j.corsci.2022.110252.
6. Trinh A. T., Nguyen T. T., Thai T. T., To T. X. H., Nguyen X. H., Nguyen A. S., Aufray M., Pébère N. - Improvement of adherence and anticorrosion properties of an epoxy-polyamide coating on steel by incorporation of an indole-3 butyric acid-modified nanomagnetite. J. Coat. Technol. Res., **13**(3) (2016) 489-499. https://doi.org/10.1007/s11998-015-9768-y.
7. Ataie A., Mostaghimi J., Pershin L., Xu P. - Fabrication of nanostructured cobalt ferrite coatings using suspension plasma spraying (SPS) technique. Surf. Coat. Technol., **328** (2017) 451-461. https://doi.org/10.1016/j.surfcoat.2017.09.003.

8. Jouyandeh M., Ganjali M. R., Ali J. A., Aghazedeh M., Stadler F. J., Saeb M. R. - Curing epoxy with electrochemically synthetized $CoxFe_3$-xO_4 magnetic nanoparticles. Prog. Org. Coat., **137** (2019) 105252. https://doi.org/10.1016/j.porgcoat.2019.105252.
9. Darmiani E., Danaee I., Rashed G. R., Zaarei D. - Formulation and study of corrosion prevention behavior of epoxy cerium nitrate-montmorillonite nanocomposite coated carbon steel. J. Coat. Technol. Res., **10**(4) (2013) 493-502. https://doi.org/10.1007/s11998-012-9463-1.
10. Trinh A. T., Thai T. T., Vu K. O., To T. X. H., Nguyen A. S., Caussé N., Pébère N. - 8-hydroxyquinoline-modified clay incorporated in an epoxy coating for the corrosion protection of carbon steel. Surf. Interfaces, **14** (2019) 26-33. https://doi.org/10.1016/j.surfin.2018.10.007.
11. Leal D. A., Kuznetsova A., Silva G. M., Tedim J., Wypych F., Marino C. E. B. - Layered materials as nanocontainers for active corrosion protection: A brief review. Appl. Clay Sci., **225** (2022) 106537. https://doi.org/10.1016/j.clay.2022.106537.
12. Barraqué F., Montes M. L., Fernández M. A., Mercader R. C., Candal R. J., Torres Sánchez R. M. - Synthesis and characterization of magnetic-montmorillonite and magnetic-organo-montmorillonite: Surface sites involved on cobalt sorption. J. Magn. Magn. Mater., **466** (2018) 376-384. https://doi.org/10.1016/j.jmmm.2018.07.052.
13. Bartonkova H., Mashlan M., Medrik I., Jancik D., Zboril R. - Magnetically modified bentonite as a possible contrast agent in MRI of gastrointestinal tract. Chem. Pap., **61**(5) (2007) 413-416. https://doi.org/10.2478/s11696-007-0057-9.
14. Kalantari K., Ahmad M. B., Shameli K., Hussein M. Z. B., Khandanlou R., Khanehzaei H. - Size-controlled Synthesis of Fe_3O_4 magnetite nanoparticles in the layers of Montmorillonite. J. Nanomater., **2014** (2014) 739485. https://doi.org/10.1155/2014/739485.
15. Zeynizadeh B., Rahmani S., Tizhoush H. - The immobilized Cu nanoparticles on magnetic montmorillonite (MMT@Fe_3O_4@Cu): As an efficient and reusable nanocatalyst for reduction and reductive-acetylation of nitroarenes with $NaBH_4$. Polyhedron, **175** (2020) 114201. https://doi.org/10.1016/j.poly.2019.114201.
16. Rafiei B., Ghomi F. A. - Preparation and characterization of the Cloisite Na^+ modified with cationic surfactants. Iran. J. Crystallogr. Mineral., **21**(2) (2013) 25-32.
17. Motte C., Poelman M., Roobroeck A., Fedel M., Deflorian F., Olivier M. G. - Improvement of corrosion protection offered to galvanized steel by incorporation of lanthanide modified nanoclays in silane layer. Prog. Org. Coat., **74** (2012) 326-333. https://doi.org/10.1016/j.porgcoat.2011.12.001.
18. Thai T. T., Trinh A. T., Olivier M. G. - Hybrid sol-gel coatings doped with cerium nanocontainers for active corrosion protection of AA2024. Prog. Org. Coat., **138** (2020) 105428. https://doi.org/10.1016/j.porgcoat.2019.105428.
19. Zhang Z. J., Chen X. Y., Wang B. N., Shi C. W. - Hydrothermal synthesis and self-assembly of magnetite (Fe_3O_4) nanoparticles with the magnetitic and electrochemical properties. J. Cryst. Growth, **310** (2008) 5453-5457. https://doi.org/10.1016/j.jcrysgro.2008.08.064.
20. Patel H. A., Somani R. S., Bajaj H. C., Jasra R. V. - Nanoclays for polymer nanocomposites, paints, inks, greases and cosmetics formulations, drug delivery vehicle and waste water treatment. Bull. Mater. Sci., **29** (2006) 133-145. https://doi.org/10.1007/BF02704606.
21. Zhu T. T., Zhou C. H., Kabwe F. B., Wu Q. Q., Li C. S., Zhang J. R. - Exfoliation of montmorillonite and related properties of clay/polymer nanocomposites. Appl. Clay Sci., **169** (2019) 48-66. https://doi.org/10.1016/j.clay.2018.12.006.
22. Allahar K. N., Orazem M. E., Ogle K. - Mathematical model for cathodic delamination using a porosity-pH relationship. Corros. Sci., **49** (2007) 3638-3658. https://doi.org/10.1016/j.corsci.2007.03.024.
23. Petrunin M. A., Maksaeva L. B., Gladkikh N. A., Yurasova T. A., Maleeva M. A., Ignatenko V. E. - Cathodic delamination of polymer coatings from metals. Mechanism and prevention methods. A review. Int. J. Corros. Scale Inhib., **10**(1) (2021) 1-28. https://doi.org/10.17675/2305-6894-2021-10-1-1.
24. Rammelt U., Reinhard G. - Application of electrochemical impedance spectroscopy (EIS) for characterizing the corrosion-protective performance of organic coatings on metals. Prog. Org. Coat., **21** (1992) 205-226. https://doi.org/10.1016/0033-0655(92)87005-U.